Available online at www.sciencedirect.com
SCIENCE DIRECT®
Applied Thermal Engineering 25 (2005) 2543–2554
APPLIED THERMAL ENGINEERING
www.elsevier.com/locate/apthermeng

Confined and unconfined FC72 and FC87 boiling on a downward-facing disc

J.C. Passos *, L.F.B. Possamai, F.R. Hirata

Universidade Federal de Santa Catarina, Departamento de Engenharia Mecânica, LABSOLAR-NCTS Cx. P. 476, 88010-900 Florianópolis S.C., Brazil

Received 1 September 2004; accepted 26 November 2004
Available online 11 February 2005

Abstract

This paper presents new results for confined and unconfined boiling of FC72 and FC87 at atmospheric pressure and low and moderate heat fluxes—lower than 45 kW/m^2—on a downward-facing disc placed at 0.2, 0.5, 1 and 13 mm distance from the base of a boiling chamber, corresponding to Bond numbers 0.28, 0.69, 1.38 and 17.95. The experimental results showed enhanced boiling as the main trend for the cases with $s = 0.2$ and 0.5 mm compared with those with $s = 1$ and 13 mm and a higher heat-transfer coefficient for FC72 boiling compared with FC87, with a wall superheating of 7.7–8 K higher for FC87.

Keywords: Boiling; Confined boiling; Bond number; Nucleate boiling; Heat transfer

1. Introduction

In many heat-transfer applications it is possible to find a large heat flux and small space for the cooling liquid. When boiling is employed as the main thermal control mechanism of a surface in a confined space its behaviour can be very different to that of the boiling in a large liquid pool and

* Corresponding author. Tel.: +55 48 331 9379; fax: +55 48 234 15 19.
E-mail address: jpassos@emc.ufsc.br (J.C. Passos).

1359-4311/$ - see front matter
doi:10.1016/j.applthermaleng.2004.11.023

Nomenclature

c_p	specific heat, J/(kg K)
C_{sf}	constant in Rohsenow's correlation
d_b	bubble diameter, m
g	acceleration due to gravity, m/s^2
h	heat-transfer coefficient, W/(m^2 K)
h_{lv}	latent vaporization heat, J/kg
k	thermal conductivity, W/(m K)
L	capillary length, m
L	characteristic length in the Nusselt and Rayleigh numbers, m
M	molar mass, kg/kmol
N	exponent of q in Eq. (4)
Pr	Prandtl number
p_r	reduced pressure
q	heat flux, W/m^2
r	exponent in Rohsenow's correlation
R_p	roughness of the heating wall, μm
s	exponent in Rohsenow's correlation
T	temperature, °C, K

Greek symbols

α	thermal diffusivity, m^2/s
β	thermal expansion coefficient, K^{-1}
μ	viscosity
v	kinematic viscosity, m^2/s
ρ	density, kg/m^3
σ	surface tension, N/m

Subscripts

l	liquid
nc	natural convection
sat	saturation
v	vapour
w	wall

can be characterized by a nucleate regime whose isolated vapor bubbles, even for a low heat flux, are difficult to maintain and become coalesced bubbles, as reported by Ishibashi and Nishikawa [1]. In order for a device or machine to work under these conditions it is necessary to find the limits of the heat flux that determine the dryout of the heating surface and the heat-transfer characteristics during the pool-boiling regime. A simple way to analyse the degree of confinement is to compute the Bond number, *Bo*, defined as the ratio between a characteristic dimension of the

confined space, s, and the capillary length, L, this latter being proportional to the vapour bubble departure diameter and calculated by

$$L = \sqrt{\frac{\sigma}{g(\rho_l - \rho_v)}} \tag{1}$$

where g, σ, ρ_l and ρ_v represent the acceleration due to gravity, the surface tension and the density of the liquid and the vapor, respectively. The Bond number is $Bo = s/L$. As a general trend, when the confined characteristic dimensions decrease, the heat-transfer coefficient increases [1–4]. When the order of magnitude of the Bond number is less than unity there is a tendency to have coalesced bubbles whereas for $Bo > 1$ the bubbles are isolated. The increase in the heat-transfer coefficient, when $Bo < 1$, is related to the evaporation of the liquid film between the flattened bubbles and the heating wall [2]. However, for $Bo < 1$, the boiling crisis is characterized by dryout and can be highly dependent on the confinement and occurs for heat fluxes that decrease with a decrease in s or Bo as reported by Katto et al. [2], Yao and Chang [3], Bonjour and Lallemand [5] and Geisler and Bar-Cohen [6]. Depending on the geometry and confinement the dryout heat flux can be of the same order of magnitude as the desired heat flux of operation [4].

The visualization of the boiling of FC72 in a confined space [4] even when the liquid is subcooled, shows coalesced bubbles blanketing the major part of the heating copper disc, when the distance (s) between the heating disc and the bottom base is 0.2 and 0.5 mm, corresponding to Bond numbers equal to 0.28 and 0.69, for heat fluxes higher than 25 kW/m^2. For subcooled boiling and s equal to 1 and 13 mm, corresponding to Bond numbers 1.38 and 17.95, and heat flux equal or less than 40 kW/m^2 the bubbles are isolated with a small number of big bubbles for the case with $s = 1$ mm.

This work presents new experimental results for confined boiling of fluorocarbons FC72 and FC87 in a reduced space between a downward-facing heating disc and the base of the boiling chamber. Particular attention is given to the heating mode.

2. Experimental set up

The test section is a copper disc with a diameter of 12 mm and thickness of 1 mm with three E thermocouples of 0.15 mm diameter set in it, close to the center of the disc, one of them being a differential type of thermocouple, and heated by an electrical resistance skin heater of 11.2 Ω bonded on the upper side of the disc. The copper disc is bonded onto a piece of PVC, beveled to an angle of 45°, with diameter 20 mm and this is mounted at the end of an aluminium tube which the thermocouple cables pass through. The test section is mounted inside a boiling chamber, consisting of a glass tube of 50 mm inside diameter and filled with a 3M dielectric fluorocarbon liquid, FC72 (C_6F_{14}) or FC87 (C_5F_{12}). Another two thermocouples are installed inside the boiling chamber. The boiling chamber is mounted inside a second chamber, 150 × 150 × 160 mm, as shown in Fig. 1, with water flowing inside whose temperature is controlled by a cryostat allowing the control of the temperature of the working fluid. The distance between the base of the boiling chamber and the copper disc is adjustable by turning the aluminium tube and controlling the distance by means of a dial indicator.

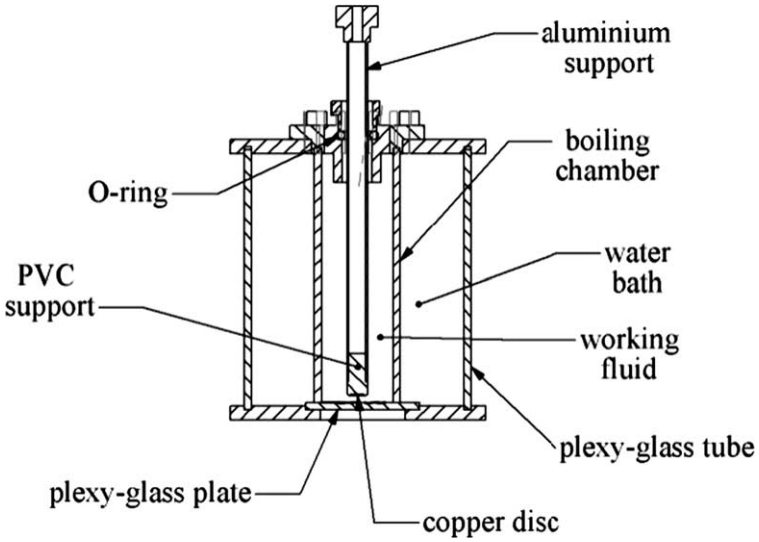

Fig. 1. Scheme of the experimental set up.

The heating disc is downward facing. The base of the boiling chamber is transparent and allows the visualisation of the boiling phenomenon. The copper surface in contact with the working fluid was polished using emery paper #600, corresponding to a roughness R_p of 1.1 μm. The tests were performed in FC72 and FC87 pools, at atmospheric pressure, at LABSOLAR/ NCTS of Federal University of Santa Catarina, in Brazil.

A DC power supply, HP6030A, is connected to the skin heater and controlled by a PC using LABVIEW and the data acquisition and preliminary treatment are carried out by a HP34970A. The heating of the disc is controlled by increasing or decreasing the heat flux.

3. Experimental procedure

The experimental procedure is programmed in LABVIEW and each average experimental point, defined by a wall temperature and a heat flux, represents a 90 s duration in the increasing mode of heating and 420 s in the decreasing mode of heating.

The temperature uncertainty is ±0.6 °C, using the same procedure reported by Passos and Reinaldo [7]. The experimental uncertainty for the heat flux is 1%, and those for the heat-transfer coefficients vary from 3% to 7% and were computed following the procedure presented by Holman [8] and Kline [9].

3.1. Single-phase natural convection

Single-phase natural convection was analysed for tests with $s = 13$ mm and the values for the heat-transfer coefficient (h_{nc}) were compared with those predicted by the following empirical correlation [10]:

$$h_{nc} = \frac{0.27Ra^{0.25}k_l}{L} \tag{2}$$

where Ra represents the Rayleigh number and is given by

$$Ra = \frac{g\beta(T_w - T_{sat})L^3}{v\alpha} \tag{3}$$

where, k_l, L, g, β, T_w, T_{sat}, v and α represent the liquid conductivity, characteristic length, acceleration due to gravity, thermal expansion coefficient, wall temperature, saturation temperature, kinematic viscosity and coefficient of diffusivity. The characteristic length L in the Nusselt and Rayleigh numbers is equal to the ratio between the surface area and the perimeter of the heating disc corresponding to a half of the radium disc. A comparison of the experimental h and the h_{nc}, Eq. (2), shows that the experimental values are higher than those calculated by Eq. (2) and the average absolute deviations are 71.3% and 67.8% for FC72 and FC87, respectively.

3.2. Heating mode

Fig. 2 shows the resulting heat flux, q, as a function of time, t, for a typical programmed LABVIEW increase in the heating function of the skin heater.

A second heating mode was tested in which, after the system rested for 90 s, the voltage was turned off for 2–3 min in order to analyse the thermal sensitivity of the system. The results obtained with the second mode were very similar to those obtained with the first and the boiling curves were obtained with a heating function without turning off the power supply, as shown in Fig. 2.

A heating function, similar to that of Fig. 2, but with a decrease in heat flux was analysed and the results for FC72 with $s = 0.2$ and 13 mm for both heating modes, increasing and decreasing, are shown in Fig. 3.

Fig. 4 shows the results for $s = 0.2$ and 13 mm for FC87. In general, the differences in the wall superheating were less than 1 K with a lower superheating for the case with decreasing heat flux.

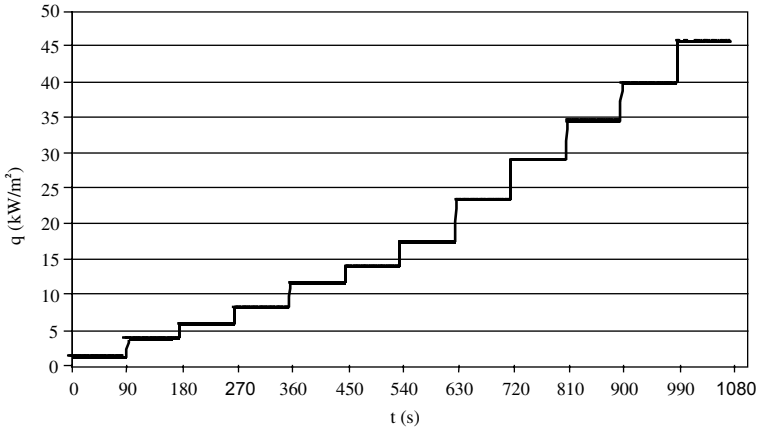

Fig. 2. A typical curve showing the increase in heat flux.

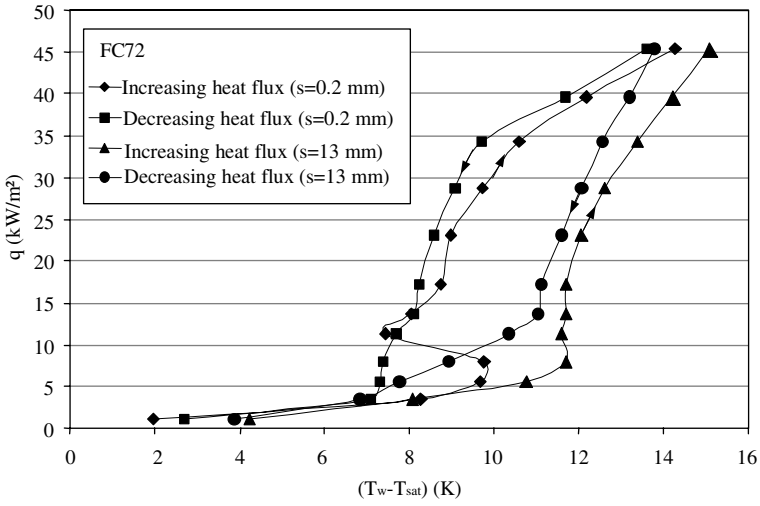

Fig. 3. Influence of the heating mode.

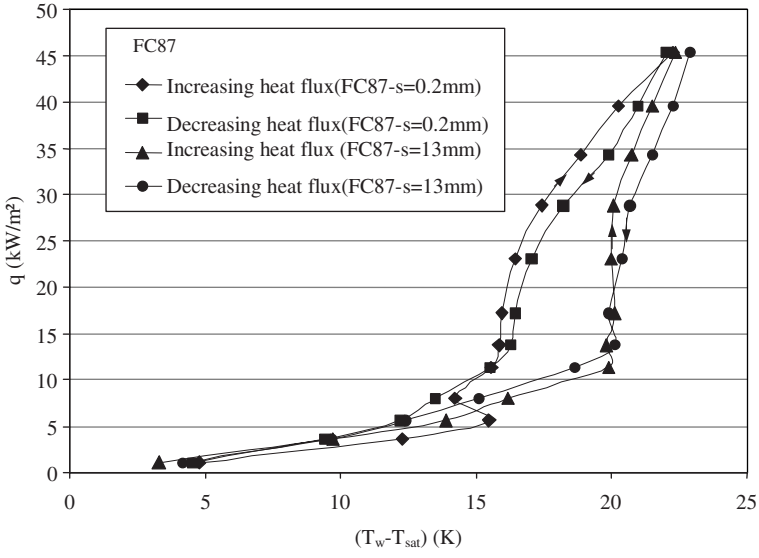

Fig. 4. Influence of the heating mode.

3.3. Relation between h and q in nucleate boiling

In order to verify the qualitative trend of the results it is interesting to analyse the relation between the heat-transfer coefficient, h, and the heat flux, as in the following equation:

$$h = Cq^n \tag{4}$$

Tables 1 and 2 present the values of n computed as a function of the experimental values for q and h, for $s = 13$ mm and FC72 and FC87, respectively. The average values of the exponent n for FC72 and FC87 are 0.732 and 0.846, respectively, with a standard deviation of 0.131 and 0.174, respectively. According to Stephan [11], n lies, in general between 0.6 and 0.8, and we can observe that only the experimental points for FC72 are within this average range.

3.4. Comparison with nucleate boiling correlations

The experimental results without confinement, $s = 13$ mm, for saturated boiling, were compared with those predicted by three correlations for nucleate boiling.

Eq. (5) is the Cooper's correlation [12]:

$$h = 55 p_r^{0.12} (-\log p_r)^{-0.55} M^{-0.5} q^{0.67} \tag{5}$$

where p_r and M are the reduced pressure and the molar mass, respectively. The exponent 0.12 of p_r is that indicated for a roughness R_p equal to 1 μm.

Eq. (6) is the Stephan–Abdelsalam's correlation [13]:

Table 1
Values for n, for saturated FC72 and $s = 13$ mm

q (kW/m^2)	h_{exp} (kW/m^{2}K)	n
13.69	1.155	1.013
17.16	1.452	0.893
23.05	1.890	0.796
28.68	2.249	0.676
34.25	2.536	0.620
39.58	2.774	0.564
45.30	2.993	0.564
Mean value		0.732
Standard deviation		0.131

Table 2
Values for n, for saturated FC87 and $s = 13$ mm

q (kW/m^2)	h_{exp} (kW/m^{2}K)	n
13.72	0.692	0.928
17.19	0.854	1.025
23.10	1.155	0.977
28.74	1.431	0.827
34.32	1.657	0.733
39.66	1.842	0.716
45.39	2.029	0.716
Mean value		0.846
Standard deviation		0.174

$$h = 207\left(\frac{k_l}{d_b}\right)\left(\frac{qd_b}{k_l T_{sat}}\right)^{0.745}\left(\frac{\rho_l}{\rho_v}\right)^{0.581} Pr_l^{0.533} R_p^{0.133} \tag{6}$$

where k_l, T_{sat}, Pr_l and R_p represent the liquid conductivity, saturation temperature in Kelvin, the liquid Prandtl number and the roughness in μm. In this correlation the characteristic length is the bubble diameter computed by

$$d_b = 0.0149\left[\frac{2\sigma}{g(\rho_l - \rho_v)}\right]^{0.5} \tag{7}$$

where θ represents the contact angle, that is recommended to be equal 35°, see [14].

Eq. (8) is the Rohsenow's correlation [15]:

$$h = \mu_l h_{lv}\left[\frac{g(\rho_l - \rho_v)}{\sigma}\right]^{1/2}\left(\frac{c_{pl}(T_w - T_{sat})}{C_{sf} h_{lv} Pr_l^s}\right)^{1/r} \tag{8}$$

where μ_l, h_{lv}, c_{pl}, T_w represent the liquid viscosity, latent vaporization heat, liquid specific heat and wall temperature, respectively. The constant C_{sf} is an experimental coefficient related to the combination of working fluid and the material heating surface, $r = 0.333$ and $s = 1.7$.

4. Results and discussion

Figs. 5 and 6 show the partial boiling curves for distances of 0.2, 0.5, 1.0 and 13 mm for FC72 and FC87, at bulk temperatures of 56 and 30 °C, respectively. The points corresponding to heat fluxes higher than 12 kW/m^2 represent the partial boiling curve for all four cases of s whereas for heat fluxes less than 5 kW/m^2 the heat-transfer mode is single phase natural convection. For heat fluxes lower than 27 kW/m^2 the wall superheating decreases with a decrease in s. For heat fluxes higher than 35 kW/m^2, with $s = 0.2$ mm, the wall temperature increases indicating the beginning

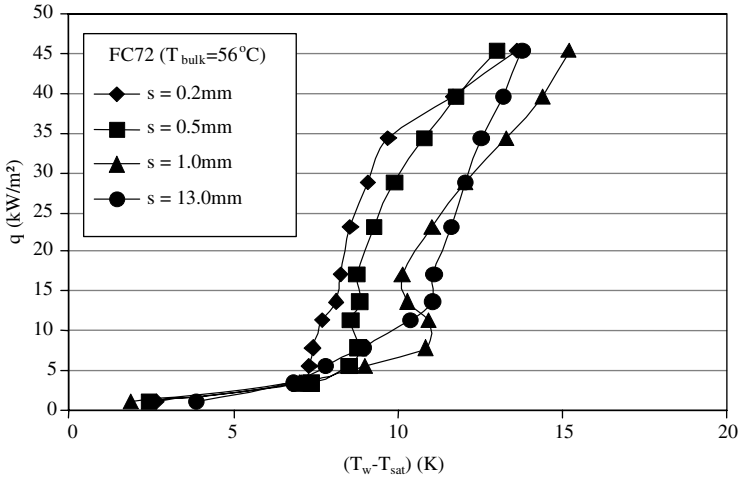

Fig. 5. Boiling curves for FC72 (T_{sat} = 56.6 °C) as a function of s with decreasing heat flux.

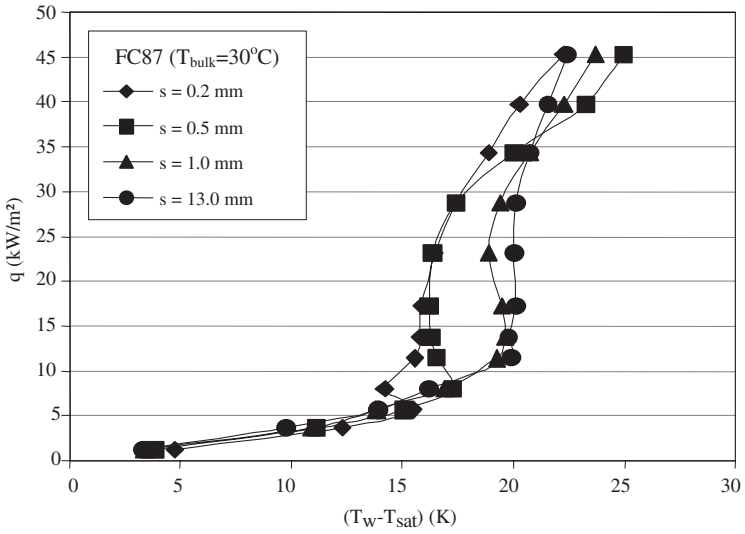

Fig. 6. Boiling curves for FC87 (T_{sat}=30 °C) as a function of s with increasing heat flux.

of the dryout and for $s = 0.5$ and 1 mm, a wall temperature increase occurs for heat fluxes higher than 30 kW/m^2. Particularly, we can observe, for heat fluxes between 12 and 40 kW/m^2, that the results for $s = 0.2$ and 0.5 mm indicate an enhanced boiling effect compared with the cases of $s = 1$ and 13 mm, as previously reported by Passos et al. [4].

Fig. 6 shows a similar trend to that shown in Fig. 5 and the partial boiling curve is represented for all cases of heat fluxes higher than 12 kW/m^2. An increase in the superheating temperature of the wall is observed in the case of $s = 0.5$ mm, for heat fluxes higher than 30 kW/m^2. For heat fluxes less than 35 kW/m^2 it is clear that the cases with higher confinement, $s = 0.2$ and 0.5 mm, whose Bond number is less than unity, show an enhancement of the boiling. As was observed in Section 1, from the visualization reported by Passos et al. [4], it can be seen that even in the case of subcooled boiling, the two-phase liquid–vapor configurations, when $s = 0.2$ and 0.5 mm, are governed by the presence of large flattened bubbles whereas for the other two confinement cases they are governed by a great number of isolated bubbles.

Figs. 7 and 8 show the boiling curves for FC72 and FC87 for $s = 0.2$ and 13 mm, respectively. In the boiling region, for $q > 10$ kW/m^2, the experimental points corresponding to the FC72 are shifted to the left in relation to those for FC87 and the wall superheating for FC87 is on average 7.7 and 8 K higher than the wall superheating for FC72 with $s = 0.2$ and 13 mm, respectively. These results indicating a higher heat-transfer coefficient for FC72 were confirmed by repetition of the tests under the same conditions.

5. Comparison of the results

Figs. 9 and 10 show the experimental heat-transfer coefficients for $s = 13$ mm and FC72 and FC87, respectively, as a function of the heat flux, and compare these results with those calculated by the correlations of Cooper, Stephan and Abdelsalam and Rohsenow. It is evident that there is

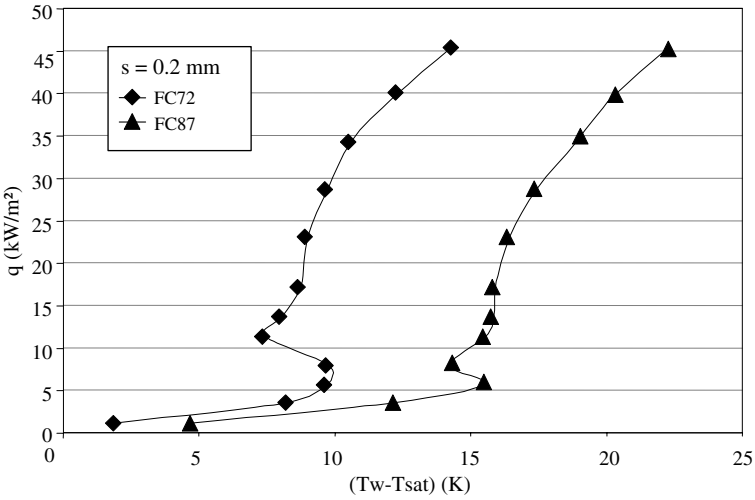

Fig. 7. Boiling curves for FC72 and FC87, for $s = 0.2$ mm.

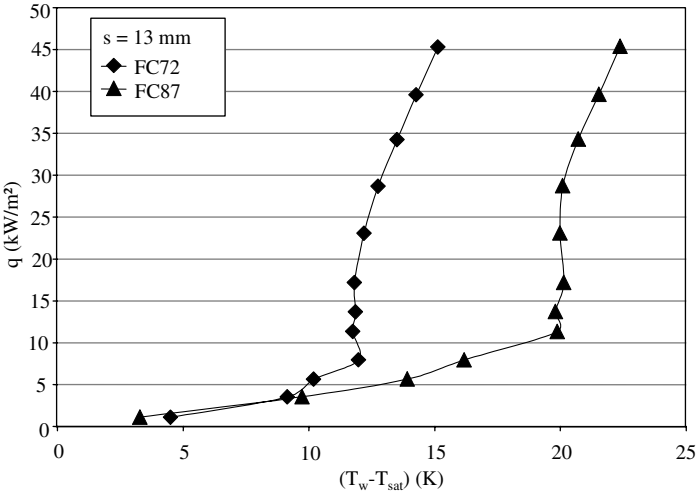

Fig. 8. Boiling curves for FC72 and FC87, for $s = 13$ mm.

non-agreement between the different correlations themselves when the fluids are FC72 and FC87. For FC72, the experimental results are within those expected according to Cooper and Stephan and Abdelsalam's correlations. The Rohsenow's correlation, with $C_{sf} = 0.0047$, fits the experimental points for $q > 25$ kW/m^2. Fig. 10 shows that for $q < 30$ kW the experimental values for h are lower than those expected from the correlations and for $q \geqslant 30$ kW/m^2 the results are 10% higher than those of Rohsenow's correlation with $C_{sf} = 0.0079$. The average values for h in Figs. 9 and 10 are 2.1 and 1.5 kW/(m^{2}K), respectively.

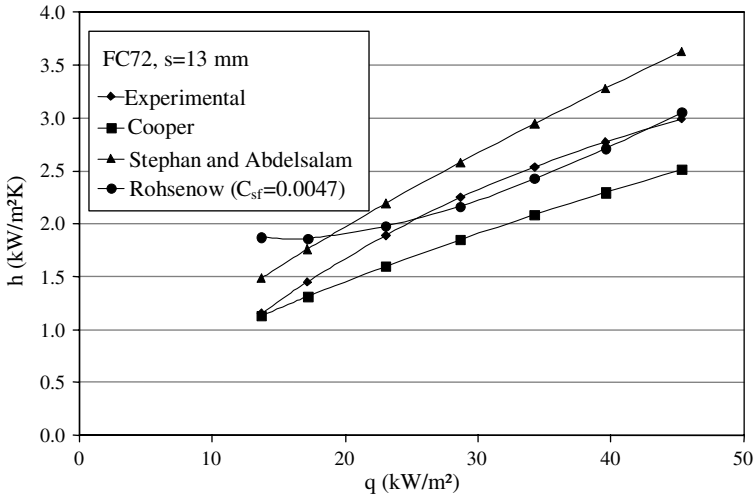

Fig. 9. Comparison between experimental data and correlations.

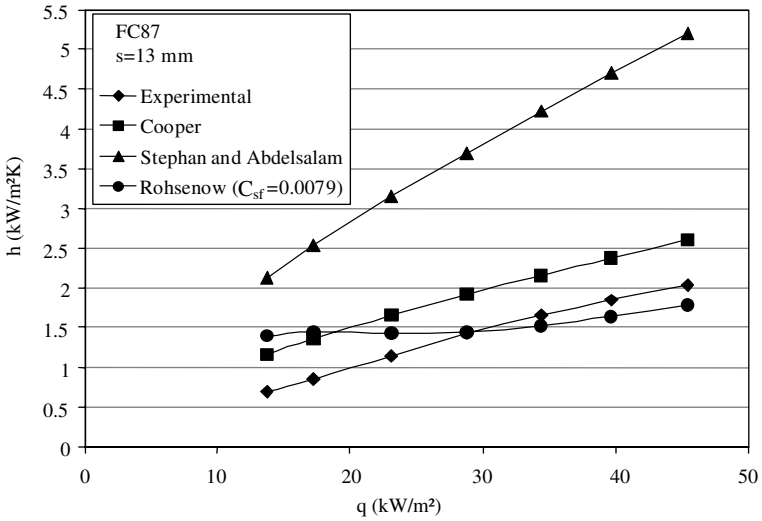

Fig. 10. Comparison between experimental data and correlations.

6. Conclusions

The following conclusions can be drawn from this study:

For Bond numbers of 0.28 and 0.69 the boiling heat-transfer coefficients are higher than those for Bond numbers of 1.38 and 17.95.

In general, for a particular confinement the heat-transfer coefficients for FC72 (C_6F_{14}) are higher than those for FC87 (C_5F_{12}) and the difference in the wall superheating varies from 7.7 to 8 K.

The empirical correlations of Cooper, Rohsenow and Stephan and Abdelsalam show non agreement between each other for FC72 and FC87.

The experimental heat-transfer coefficient and the heat flux are related by a power law whose average exponents of q for FC72 and FC87 are 0.732 and 0.846, respectively.

Acknowledgements

The authors are grateful for the support of Brazilian Space Agency (AEB) and the Research Council of Brazil (CNPq) in performing this study. The authors extend their thanks to 3M (Italy) for the donation of FC72 and FC87 and to Mr. Eduardo Ludgero da Silva for his support in the laboratory.

References

[1] E. Ishibashi, K. Nishikawa, Saturated boiling heat transfer in narrow spaces, Int. J. Heat Mass Transfer 12 (1969) 863–894.
[2] Y. Katto, S. Yokoya, K. Teraoka, Nucleate and transition boiling in a narrow space between two horizontal, parallel disk surfaces, Bull. JSME 20 (143) (1977) 638–643.
[3] S.C. Yao, Y. Chang, Pool boiling heat transfer in a confined space, Int. J. Heat Mass Transfer 26 (6) (1983) 841–848.
[4] J.C. Passos, F.R. Hirata, L.F.B. Possamai, M. Balsamo, M. Misale, Confined Boiling of FC72 and FC87 on a Downward facing heating copper disk, Int. J. Heat Fluid Flow 25 (2) (2004) 313–319.
[5] J. Bonjour, M. Lallemand, M. Effects, of confinement and pressure on critical heat flux during natural convective boiling in vertical channels, Int. Commun. Heat Mass Transfer 24 (2) (1997) 191–200.
[6] K.J.L. Geisler, A. Bar-Cohen, Nucleate pool boiling heat transfer in narrow vertical channels, Proceedings of the Fifth Int. Conference on Boiling Heat Transfer, Session XII, Montego Bay, Jamaica, University of Florida, 5p, 2003.
[7] J.C. Passos, R.F. Reinaldo, Analysis of pool boiling within smooth and grooved tubes, ETFS—Exp. Thermal Fluid Sci. 22 (2000) 35–44.
[8] J.P. Holman, Experimental Methods for Engineers, fifth ed., McGraw-Hill, 1989.
[9] S.J. Kline, The purposes of uncertainty analysis, ASME J. Fluid Eng. 107 (1985) 153–160.
[10] F.P. Incropera, D.P. DeWitt, Fundamentos de Transferência de Calor e de Massa, fourth ed., LTC Editora, Rio de Janeiro-RJ, p. 271, 1996 (in Portuguese).
[11] K. Stephan, Heat Transfer in Condensation and Boiling, Springer-Verlag, New York, 1992, p. 141.
[12] M.G. Cooper, Saturation nucleate pool boiling: a simple correlation, First U.K. National Conference on Heat Transfer, in: I. Chemical E. Symposium Series No. 86, 1984, pp. 785–793.
[13] K. Stephan, M. Abdelsalam, Heat transfer correlations for natural convection boiling, Int. J. Heat Mass Transfer 23 (1980) 73–87.
[14] V.P. Carey, Liquid–Vapor Phase-Change Phenomena, Taylor & Francis, 1992.
[15] G. Hewitt, Boiling, in: W.M. Rohsenow, J.P. Hartnett, Y.I. Cho (Eds.), Handbook of Heat Transfer, third ed., McGraw Hill, New York, 1998, pp. 15.46–15.47 (Chapter 15).